RESEARCH ARTICLE OPEN ACCESS

# Methodology for Obtaining Speckle Interferometry through Lateral and Angular Displacement

Josué del Valle-Hernández*, J. Felix López Rocha**, Alejandro García Trujillo**, José Alfredo Gasca González**, Adrian Pérez-Benavidez***, Edgardo Picon Rodríguez****, Mauricio Valtierra Domínguez****and F.Alejandro Ramírez Díaz****

* (Dept. of Divison of Postgraduate Studies and Investigation, Tecnológico Nacional de México, Campus León
Email: josue.delvalle@leon.tecnm.mx
** (Dept. of Basic Sciences, Tecnológico Nacional de México, Campus León
*** (Dept. of Metrology and Quality control, Instituto Politécnico Nacional, Campus León
**** (Dept. of Metal-Mechanical, Tecnológico Nacional de México, Campus León

----------**********----------

## Abstract:

Interferometry is a highly useful tool in metrology, and speckle interferometry allows for measurements with micrometer-level resolution. In the following pages of this document, the standard technique or methodology will be presented to obtain interference fringes caused by lateral or angular displacement. That is, a diffractive element (such as a negative or photographic film) can be obtained by taking a double exposure photograph of an object in an initial position and then in a second position, thus causing a displacement. When this grating is illuminated with a laser beam and aided by an optical system, interference fringes can be observed on a screen. The position, thickness, and spacing of these fringes provide the necessary information to calculate the lateral or angular displacement.

*Keywords* **— microonda, interferómetro de young.**

----------**********----------

## I. INTRODUCTION

When a rough surface is illuminated by a laser beam, an image with bright dots can be observed. Upon closer inspection, a speckled pattern appears superimposed on the image. This type of pattern is visible even when the surface is not in focus. Although this effect complicates the task of photographing rough objects with coherent light, it is a valuable source of information regarding the mechanical properties of the observed surface.

There are speckle-based methods that allow the measurement of deformations, displacements, rotations, vibration amplitudes, and more. These methods are often less demanding than holographic interferometry, since some of the factors that limit holography enhance speckle-based techniques.

Objective speckle can be seen in the following figure, which shows a rough surface illuminated by an expanded laser beam and a screen that captures the light scattered by the surface. The screen reveals a granular or speckled pattern once again.

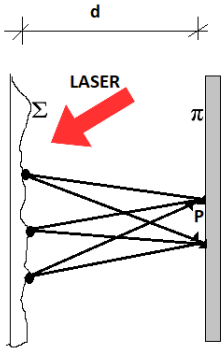


Fig. 1. Objective Speckle schematic diagram.

Subjective speckle occurs when a camera or the human eye focuses on a rough surface illuminated by a laser beam. A speckled pattern also appears. In this

  

case, the observed speckle corresponds to the diffraction of the field at the system's aperture, and the average speckle size is given by:

$$\frac{z\lambda}{D} \tag{1}$$

where $z$ is the distance from the aperture to the image plane, λ is the laser wavelength, and $D$ is the aperture diameter.

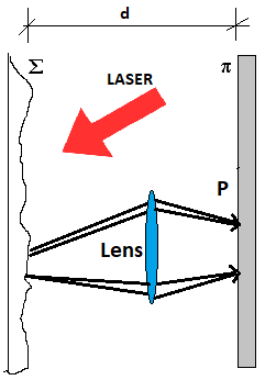


Fig. 2. Subjective Speckle schematic diagram.

If the speckle is observed in the focal plane of a converging lens, the average size is modified accordingly.

$$\frac{f\lambda}{D} = A\lambda \tag{2}$$

When certain transformations are applied to the surface (e.g., parallel translation, normal rotation), both subjective and objective speckle patterns shift accordingly.

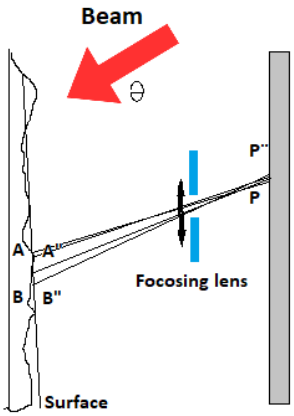


Fig. 3. Speckle schematic diagram.

In the image plane, the speckle pattern shifts.

$$d_z^{z'} \tag{3}$$

In the focal plane, a rotation results in displacement as well.

$$-(1+\cos(q))gf \tag{4}$$

Two speckle patterns are captured and illuminated. The displacement causes the appearance of interference fringes, whose spacing is inversely proportional to the magnitude of the displacement.

In effect:

$$\begin{aligned} & u(k_x,k_y) \\ & = \sum e(x,y)\, e^{i*k_x*x+i*k_y*y} \\ & + e^{i*k_x*d} \sum e(x,y)\, e^{i*k_x*x+i*k_y*y} \\ & = E(k_x,k_y)(1+\cos(k_x d)+i*sen(k_x)*d) \end{aligned} \tag{5}$$

## II. EXPERIMENTAL DEVELOPMENT

First, all the necessary components and materials were gathered in order to proceed with the assembly of our experiment. The materials provided for the execution of the experiment were:

- He-Ne laser (632.8 nm).
- Shutter and trigger.
- Mechanical mounts with micrometric adjustment (translation and angular).
- Spatial filter with a 20X microscope objective and small aperture (pinhole).
- Film camera with "Technical Pan" film and trigger.
- Converging lens with a focal length of approximately 85 cm.
- Transmission (ground glass) or reflection screen.
- Measuring tape.
- Close-up lenses.

LATERAL DISPLACEMENT

  

To create the diffractive element (speckle-patterned negative), it is necessary to obtain a double-exposure photograph of the object—first in its initial position, and then in a second position after a micrometric lateral displacement. To do this, the experimental setup shown in the following figure was assembled:

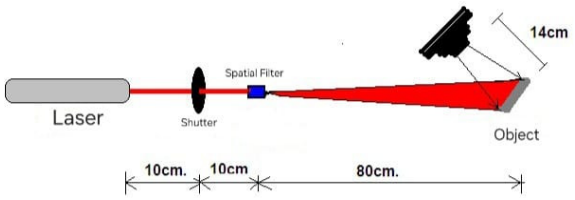


Fig. **4**. Experimental setup for obtaining double-exposure photographs to create the diffractive element.

Before taking the double-exposure photographs of the object, it was necessary to take several test photographs of the object (a metal plate) using different exposure times in order to determine the optimal exposure time for creating the diffractive element.

To capture these photographs, the object was focused using close-up lenses, as the minimum focusing distance of the provided camera was 45 cm. Therefore, close-up lenses 1 and 2 were added to the camera lens, reducing the focusing distance to 14 cm. Close-up lens 3 was not used because it would have brought the metal plate (object) too close to the camera, potentially obstructing the path of the spatially filtered beam.

An advantage of using a 20X microscope objective instead of a 40X one for spatial filtering was also observed: the laser beam remains narrower, allowing a shorter distance between the object and the camera.

Another consideration for focusing on the camera was the use of a reference marker. In our case, a circular stamp was affixed to the metal plate. Proper focus was confirmed when this stamp appeared aligned both horizontally and vertically, as shown in the following figure:

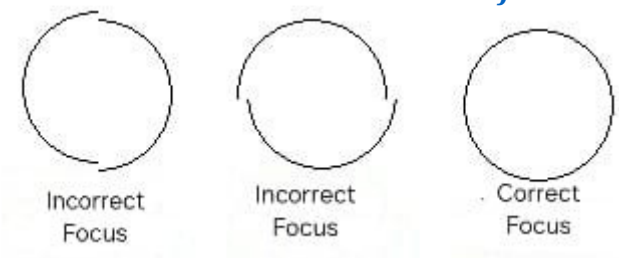


Fig. 5. Correct and incorrect focus using a circular stamp as reference.

Once the camera was properly focused, photographs were taken at various exposure times. These were then developed to obtain the negatives. Each negative was analyzed for contrast, and based on the results, an optimal exposure time of 2 seconds was selected for the double exposure. This is summarized in the following table:

| Num. Photography | Exposition time (s) |
|---|---|
| 1 | 1 |
| 2 | 2 |
| 3 | 3 |
| 4 | 4 |
| 5 | 6 |

Table. 1. Photographs taken at various exposure times.

To carry out the double exposure, the following methodology was followed:

- With the setup as shown in Figure 1, and in complete darkness, the camera was triggered, leaving the shutter open using the mechanical trigger.
- The shutter was opened for 1 second.
- The metal plate (object) was laterally displaced using the micrometer, by a distance within the range of 100 to 200 µm.
- The shutter was opened again for 1 second, completing the 2-second double exposure.
- The camera shutter was closed using the trigger.
- The film was developed using the standard photographic process.
- The result was the diffractive element (speckled negative).

  

This methodology was applied multiple times to obtain diffractive elements corresponding to various lateral displacements applied to the metal plate. These displacements are presented in the following table:

| Num. Photography | Displacement (µm) |
|---|---|
| 1 | 100 |
| 2 | 120 |
| 3 | 140 |
| 4 | 160 |
| 5 | 180 |
| 6 | 200 |

Table. 2. Photo session showing the lateral displacements applied to the object.

To observe the interference fringes on a screen, the following experimental setup was assembled:

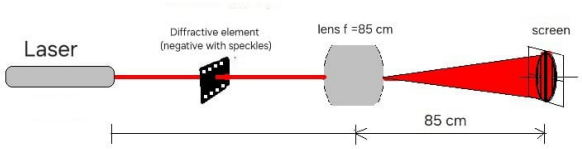


Fig. **6**. Experimental setup to observe interference fringes on a screen for fringe spacing measurements.

With the setup shown in Figure 3, the interference fringes can be projected onto a screen, allowing for physical measurements of fringe thickness and spacing. These measurements contain the necessary data to calculate the displacement applied to the object from its initial position using the following formula:

$$S = \frac{\lambda * m}{d} \quad (7)$$

Where:

- $S$ = Displacement
- $\lambda$ = Wavelength
- $m$ = Magnification
- $d$ = Fringe spacing

To determine the magnification factor (m), the circular stamp affixed to the object was used as a reference. The stamp's actual diameter was 13 mm, and it measured 4.5 cm on the negative. The ratio yielded a magnification of:

$$m = \frac{4.5\ cm}{1.3\ cm} \approx 2.88$$

A second measurement was performed to validate the magnification factor. A 10 mm mark on the object corresponded to 3.5 cm on the negative, which also gave:

$$m = \frac{3.5\ cm}{1.0\ cm} \approx 2.88$$

This method allows for the calculation of an object's lateral displacement. The interpretation of the interference fringes and the resulting values of SSS will be discussed later in the Results section.

ROTATIONAL DISPLACEMENT

The methodology for this section is very similar to that of lateral displacement, with the difference being that the object undergoes a rotational displacement in a plane, applied via a micrometer that rotates a graduated disk by a small angle. The experimental setup was modified as follows:

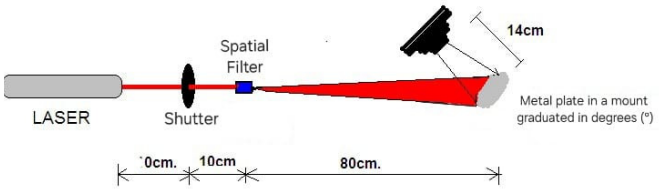


Fig. 6. Experimental setup for obtaining double-exposure photographs to create the diffractive element (rotational displacement).

The focusing procedure for the camera remained the same as described earlier (see Fig. 2). In practice, the setup was unchanged except that the object with lateral displacement was replaced by one undergoing rotational displacement, with all other components remaining in place.

As before, multiple photographs of the object were taken. The negatives were developed, and their contrast was analysed to determine the optimal exposure time. The best exposure time was found to be 8 seconds, meaning a total double exposure time

  

of 8 seconds. The various exposure times tested are listed in the following table:

| Num. Photography | Exposition time (s) |
|---|---|
| 1 | 1 |
| 2 | 2 |
| 3 | 4 |
| 4 | 8 |

Table. 3. Photo session at various exposure times to determine the optimal time.

The following methodology was followed to perform the double exposure:

- With the setup shown in Figure 4, and in complete darkness, the camera was triggered, leaving the shutter open using the mechanical trigger.
- The shutter was opened for 4 seconds.
- The metal plate (object) was rotated using the micrometer, which rotated the graduated disk by a small angle, within the range of 0.05º to 0.25º.
- The shutter was opened again for 4 seconds, thus completing the 8-second double exposure.
- The camera shutter was closed using the trigger.
- The film was developed using the standard photographic process.
- The result was the diffractive element (speckled negative).

This methodology was applied multiple times to obtain diffractive elements corresponding to various rotational displacements applied to the metal plate. These displacements are listed in the following table:

| Num. Photography | Angular Displacement (°) | Exposition time (s) |
|---|---|---|
| 1 | 0.05 | 8 |
| 2 | 0.10 | 8 |
| 3 | 0.15 | 8 |
| 4 | 0.20 | 8 |
| 5 | 0.25 | 8 |

Table. 4. Photo session showing the lateral displacements applied to the object.

Similarly, using the setup described in Figure 3, the interference fringes can be projected onto a screen. This allows for physical measurements of the fringe spacing and thickness, which provide the necessary information to determine the rotational displacement applied to the object from its initial position.

## III. RESULTS

LATERAL DISPLACEMENT IN A PLANE

The following photographs were obtained via **reflection** of the **interference fringes**:

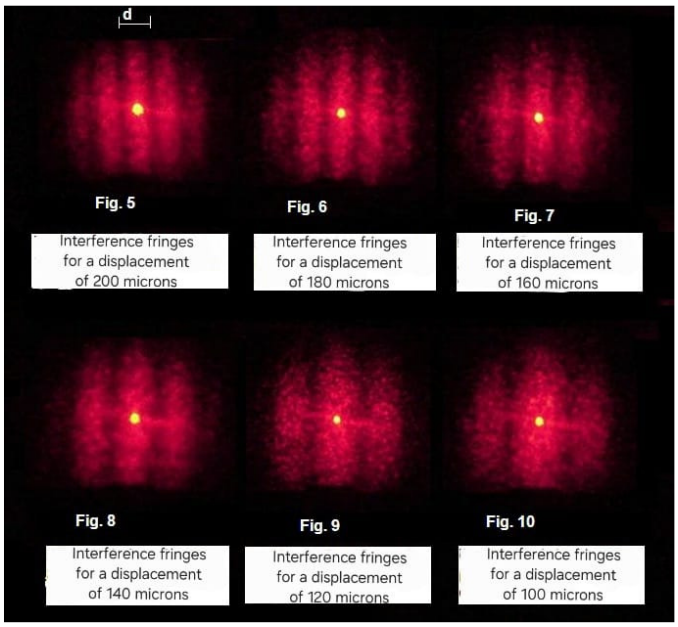


To calculate the experimental displacement, the following equation was used:

$$S = \frac{m * f}{d}$$

Where:

S = displacement
λ = wavelength
m = magnification
d = fringe spacing
f = focal length of the lens

f = 85 cm
λ = 632.8 nm
m = 2.88

The results can be seen in the following table:

  

| Theoretical Displacement (µm) | d (mm) | Experimental Displacement (µm) |
|---|---|---|
| 100 | 18 | 103 |
| 120 | 15.5 | 120 |
| 140 | 13 | 143 |
| 160 | 12 | 156 |
| 180 | 9.5 | 186 |
| 200 | 9 | 207.5 |

ROTATIONAL DISPLACEMENT IN A PLANE

The first attempt failed; it was not possible to observe interference fringes for the displacements shown in Table 4. This was due to the fact that, during the double exposure process, I accidentally moved the rotating plate, causing motion in the opposite direction of the intended displacement. Additionally, having to handle both the camera's diaphragm and the shutter by myself in complete darkness increased the risk of error.

Therefore, I conducted another double exposure photo session with the characteristics shown in the following table:

| Num. Photography | Angular Displacement (°) | Exposition time (s) |
|---|---|---|
| 1 | 0.05 | 8 |
| 2 | 0.10 | 8 |
| 3 | 0.15 | 8 |

Table 5. Measurements taken from the experimental setup of the Michelson interferometer for microwaves.

The following photographs were then obtained by reflecting the interference fringes:

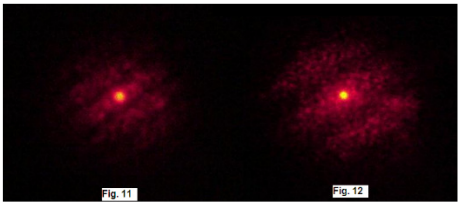


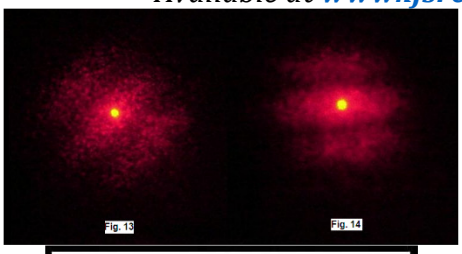


Fig. 11 Interference fringes for a rotational displacement of 0.05°

Fig. 12 Interference fringes for a rotational displacement of 0.1°

Fig. 13 Interference fringes for a rotational displacement of 0.15°

Fig. 14 Interference fringes for a rotational displacement of 0.2°

## IV. CONCLUSIONS

During the setup of the experimental arrangement, the advantage of using a 20x objective instead of a 40x for spatial filtering was observed, as the beam did not diverge excessively. This allowed the distance between the object and the camera to be reduced.

It was observed that the fringe spacing is inversely proportional to the lateral displacement applied to the object; that is, the smaller the lateral displacement, the greater the separation between interference fringes. The reliability of the equation $S = \frac{\lambda * f}{m * d}$ was confirmed and deduced by comparing theoretical and experimental displacements. It was verified that when there is lateral displacement of an object, the interference fringes are perpendicular to that displacement.

In the case of rotational displacement, if the negative (diffractive element) is moved horizontally, the spacing and thickness of the interference fringes also vary. This spacing increases when the laser beam is closer to the center and decreases as the laser beam moves away from the center. This is logical since the spacing is proportional to the radius.

Similarly, for negatives with rotational displacement, if the laser beam shifts vertically across the negative, the interference fringes tend to rotate, meaning they will have an inclined alignment. In other words, the fringes vary depending on the position where the beam strikes the image formed on the negative.

  

Interferometry is a very useful tool in metrology; with techniques such as Speckle, it is possible to perform measurements with micro-level precision.

## REFERENCES

[ 1 ] Sirohi, R. S. (Ed.). (1993). Speckle metrology (1ª ed.). Marcel Dekker Inc.

[ 2 ] Jones, R., & Wykes, C. (1983). Holographic and speckle interferometry: A discussion of the theory, practice and application of the techniques (1ª ed.). Cambridge University Press.

[ 3 ] Jones, R., & Wykes, C. (1989). Holographic and speckle interferometry (2ª ed.). Cambridge University Press.

[ 4 ] Scientific American – The Amateur Scientist. (1972, February). Speckle interferometer. Scientific American.

[ 5 ] Hecht, E. (2002). Optics (4ª ed.). Addison-Wesley.

[ 6 ] Vest, C. M. (1979). Holographic interferometry. Wiley-Interscience

  